Symmetry of Nanotubes

M. Damnjanović,† T. Vuković, and I. Milošević
Faculty of Physics, University of Belgrade, POB 368, Belgrade 11001, Yugoslavia

(Dated: May 9, 2000)

Nanotubes have become one of the most attractive subjects in solid state physics owing to their potential applications in nanotechnology. Due to their emphasized symmetry, the group theory appears as one of the important tools in theoretical investigations of nanotubes. Here we present a short review of the basic symmetry methods in the physics of nanotubes.

PACS numbers: 61.46.+w,78.66.-w,63.20.-e

During my studies in early seventies at the Faculty of Physics in Belgrade Marko Jarić was one of the older colleagues. Whenever something seemed difficult to understand he was the person to ask for help. His influence on the Belgrade school of physics continued after he went to USA. In particular, his work and results in the applications of the symmetry in physics inevitably increased the interest for the subject here. This paper is a compilation of some of our recent results in symmetry of nanotubes. Section IV is connected to the Marko's research of Molien functions[1]. (M.D.)

I. INTRODUCTION

The single-wall carbon nanotubes (SWCT) are quasi 1D cylindrical structures[2,3,4], which can be imagined as rolled-up cylinders of the 2D honeycomb lattice of the single atomic layer of crystalline graphite. Frequently, several single-wall tubes are coaxially arranged, making multi-wall nanotubes. Since their diameters are small (down to 0.7 nm) in comparison to lengths (up to tens of μm), the theoretical model of the extended (i.e. infinite, and hence without caps at the ends) nanotube is well justified. After the discovery of carbon nanotubes, a variety of tubular quasi 1D crystals with different constituents, but with similar geometry have been reported: BN, $B_xC_yN_z$, MoS_2, WS_2, etc.

The pronounced symmetry of nanotubes is obviously relevant to both the deep insight into the physical properties (quantum numbers, selection rules, optical activity, conducting properties, etc.) and easier calculations. Therefore, the symmetry studies have accompanied the research of SWCT from their discovery. They started by the classification of the graphene tubes according to the fivefold, threefold or twofold axis of the related C_{60} molecule[5], and gave just a part of their point group symmetry. The translational periodicity was discussed in context of the nanotube metallic properties[6]. More recently, the helical and rotational symmetries were found[7,8]: the screw axis was characterized in terms of the tube parameters, as well as the order of the principle rotational axis[8]. This task has been completed recently[9,10]: the full geometric symmetry of the extended single-wall nanotubes has been described by the line groups.

On the other hand, the symmetries of neither the double- and multi-wall tubes nor of the tubes with different elements have ever been seriously studied, despite their importance for applications in nanodevices. Here we present the exhaustive list of symmetries of such tubes.

In Section II a reminder on the line groups is given. Then, in Section III the line groups of nanotubes are derived: the familiar symmetries of the original honeycomb lattice are transferred into the tubular geometry and those which remain symmetries of the rolled up lattice form the corresponding line group of the SWCT. Besides the rotational, translational and helical symmetries (usually used in literature), the horizontal U axes and, for the zig-zag and the armchair tubes, the mirror- and glide-planes are also present. This concept is easily generalized to other types of the single wall tubes. The symmetry groups of multi-wall carbon nanotubes (these are either line groups or axial point groups) are studied in Subsection III C. Note that among them are also the tubes not translationally periodic.

Many of the physical properties of nanotubes are determined by their symmetry. Firstly, there are properties characterized by the second rank tensors; these tensors have already been found[11], and a typical study of this type[10] yields exaustive classification of different types of optical activity of nanotubes, with the optic axes and the corresponding examples. Also, the assignation of the tight-binding electronic bands by the symmetry based quantum numbers has been performed[12]. The general forms of the potentials for various problems in nanotube physics are derived in Section IV. They are applied in discussion of the relative positions of the components in the multi-wall tubes, and the structure of the local current density.

II. LINE GROUPS

The line groups[13,14] contain all the symmetries of the systems periodical in one direction and usually are used in the context of stereoregular polymers and quasi-1D subsystems of 3D crystals. It immediately follows that, being periodic along its axis, any extended single-wall nanotube has the symmetry described by one of the line groups.

All line group transformations leave the tube axis (z-axis, by convention) invariant. Consequently, such a transformation $(P|t)$ (Koster-Seitz symbol) is some point group operation P preserving the z-axis, followed by the translation for t along the z-axis. Action on the point $\mathbf{r} = (x, y, z)$ gives $(P|t)\mathbf{r} = (x', y', z')$ with

$$x' = P_{xx}x + P_{xy}y, \quad y' = P_{yx}x + P_{yy}y, \quad z' = P_{zz}z + t. \tag{1}$$

Here, P_{ij} are elements of the 3×3 matrix of P in the Cartesian coordinates. Those elements coupling z to the other axes vanish; such point operations are called axial and they form seven types of the axial point groups[15]: $\mathbf{C_n}$, $\mathbf{S_{2n}}$, $\mathbf{C_{nh}}$, $\mathbf{C_{nv}}$, $\mathbf{D_n}$, $\mathbf{D_{nd}}$, $\mathbf{D_{nh}}$, where $n = 1, 2, \ldots$ is the order of the principle rotational axis.

There are infinitely many line groups, since there is no crystallographic restriction on the order of the principle axis, and they are classified within 13 families (Table I). Each line group is a product $\mathbf{L} = \mathbf{ZP}$ of one axial point group $\mathbf{P}$ and one infinite cyclic group $\mathbf{Z}$ of the generalized translations (screw-axis $\mathbf{T}_q^r$, pure translations $\mathbf{T} = \mathbf{T}_1^0$, or glide plane $\mathbf{T}_c$, generated by the transformations $(I|a)$, $(C_q^r|\frac{n}{q}a)$ and $(\sigma_v|\frac{a}{2})$, respectively[16]). Thus, to determine the full symmetry of a nanotube, both of these factors (having only the identical transformation in common) should be found. The point factor $\mathbf{P}$ should be distinguished from the isogonal point group $\mathbf{P}_I$ of the line group[14]: only for the symorphic groups, when $\mathbf{Z} = \mathbf{T}$, these groups are equal; otherwise $\mathbf{P}_I$ is not a subgroup of $\mathbf{L}$. Due to the convention[16], $2\pi/q$ is the minimal angle of rotation performed by the elements of the line group (if the screw axis is nontrivial, it is followed by some fractional translation), as well as by its isogonal point group.

The easiest way to determine the line group $\mathbf{L}$ of a system is to find firstly the subgroup $\mathbf{L}^{(1)}$, containing all the translations and the rotations around the principle axis (including the ones followed by fractional translations). Having the same screw axis ($\mathbf{T}$ is a special case) as $\mathbf{L}$, and the same order n of the principle axis, this subgroup $\mathbf{L}^{(1)} = \mathbf{T}_q^r\mathbf{C}_n$ is the maximal subgroup from the first line group family. Then the symmetries complementing $\mathbf{L}^{(1)}$ to $\mathbf{L}$ should be looked for. To complete $\mathbf{Z}$, it should be checked if there is a vertical glide plane. Also, $\mathbf{C}_n$ is to be complemented to $\mathbf{P}$ by eventual additional point group generators; at most two of them are to be chosen among the mirror planes, horizontal rotational axes of order two or rotoreflection axis (refining pure rotations that are already encountered in $\mathbf{C}_n$).

TABLE I: **Line groups.** *For each family of the line groups the international symbol, different factorizations, the maximal first family subgroup and isogonal point group P_I, are presented (n is the order of the principle rotational axis of P_I). Here, $\mathbf{T}_{cd}$ denotes the glide plane bisecting the angle between vertical mirror planes in P. For the groups of the families 1 and 5, q is multiple of n (p from the international symbol is function of n, q and r).*

	International symbol		Factorizations	$\mathbf{L}^{(1)}$	P_I
	n even	n odd			
1	$\mathbf{L}q_p$		$\mathbf{T}_q^r \otimes \mathbf{C}_n$	$\mathbf{T}_q^r \otimes \mathbf{C}_n$	$\mathbf{C}_q$
2	$\mathbf{L}(2n)$	$\mathbf{L}\bar{n}$	$\mathbf{T} \wedge \mathbf{S}_{2n}$	$\mathbf{T} \otimes \mathbf{C}_n$	$\mathbf{S}_{2n}$
3	$\mathbf{L}(2n)$	$\mathbf{L}n/m$	$\mathbf{T} \wedge \mathbf{C}_{nh}$	$\mathbf{T} \otimes \mathbf{C}_n$	$\mathbf{C}_{nh}$
4	$\mathbf{L}(2n)_n/m$		$\begin{matrix}\mathbf{T}_{2n}^1\mathbf{C}_{nh} \\ \mathbf{T}_{2n}^1\mathbf{S}_{2n}\end{matrix}$	$\mathbf{T}_{2n}^1\mathbf{C}_n$	$\mathbf{C}_{2nh}$
5	$\mathbf{L}q_p22$	$\mathbf{L}q_p2$	$\mathbf{T}_q^r \wedge \mathbf{D}_n$	$\mathbf{T}_q^r \otimes \mathbf{C}_n$	$\mathbf{D}_q$
6	$\mathbf{L}nmm$	$\mathbf{L}nm$	$\begin{matrix}\mathbf{T}\otimes\mathbf{C}_{nv} \\ \mathbf{C}_{nv}\wedge\mathbf{T}_{cd}\end{matrix}$	$\mathbf{T} \otimes \mathbf{C}_n$	$\mathbf{C}_{nv}$
7	$\mathbf{L}ncc$	$\mathbf{L}nc$	$\mathbf{C}_n \wedge \mathbf{T}_c$	$\mathbf{T} \otimes \mathbf{C}_n$	$\mathbf{C}_{nv}$
8	$\mathbf{L}(2n)_nmc$		$\begin{matrix}\mathbf{C}_{nv}\wedge\mathbf{T}_{2n}^1 \\ \mathbf{C}_{nv}\wedge\mathbf{T}_{cd}\end{matrix}$	$\mathbf{T}_{2n}^1 \otimes \mathbf{C}_n$	$\mathbf{C}_{2nv}$
9	$\mathbf{L}(\bar{2n})2m$	$\mathbf{L}\bar{n}m$	$\begin{matrix}\mathbf{T}\wedge\mathbf{D}_{nd} \\ \mathbf{T}_c\wedge\mathbf{D}_{nd}\end{matrix}$	$\mathbf{T} \otimes \mathbf{C}_n$	$\mathbf{D}_{nd}$
10	$\mathbf{L}(\bar{2n})2c$	$\mathbf{L}\bar{n}c$	$\mathbf{T}_c\mathbf{S}_{2n} = \mathbf{T}_{cd}\mathbf{D}_n$	$\mathbf{T} \otimes \mathbf{C}_n$	$\mathbf{D}_{nd}$
11	$\mathbf{L}n/mmm$	$\mathbf{L}(\bar{2n})2m$	$\begin{matrix}\mathbf{T}\wedge\mathbf{D}_{nh} \\ \mathbf{T}_c\mathbf{D}_{nh}\end{matrix}$	$\mathbf{T} \otimes \mathbf{C}_n$	$\mathbf{D}_{nh}$
12	$\mathbf{L}n/mcc$	$\mathbf{L}(\bar{2n})2c$	$\mathbf{T}_c\mathbf{C}_{nh} = \mathbf{T}_c\mathbf{D}_n$	$\mathbf{T} \otimes \mathbf{C}_n$	$\mathbf{D}_{nh}$
13	$\mathbf{L}(2n)_n/mcm$		$\begin{matrix}\mathbf{T}_{2n}^1\mathbf{D}_{nh}=\mathbf{T}_{2n}^1\mathbf{D}_{nd} \\ \mathbf{T}_c\mathbf{D}_{nh}=\mathbf{T}_c\mathbf{D}_{nd}\end{matrix}$	$\mathbf{T}_{2n}^1 \otimes \mathbf{C}_n$	$\mathbf{D}_{2nh}$

III. SYMMETRY OF NANOTUBES

A Single-wall carbon nanotubes

Elementary cell of the hexagonal honeycomb lattice (Fig. 1) is formed by the vectors $\vec{a}_1$ and $\vec{a}_2$ of the length $a_0 = 2.461$Å; within its area $S_g = \sqrt{3}/2a_0^2$ there are two carbon atoms at positions $(\vec{a}_1 + \vec{a}_2)/3$ and $2(\vec{a}_1 + \vec{a}_2)/3$. The single-wall nanotube (n_1, n_2) is formed when the honeycomb lattice is rolled up in such a way that the chiral vector $\vec{c} = n_1\vec{a}_1 + n_2\vec{a}_2$ becomes the circumference of the tube (its end and origin match). The tubes $(n_1, 0)$ and (n_1, n_1) are called zig-zag ($\mathcal{Z}$) and armchair ($\mathcal{A}$), respectively, while the others are known as the chiral ($\mathcal{C}$) ones. The chiral angle θ of the nanotube is the angle between the chiral vector $\vec{c}$ and the zig-zag direction $\vec{a}_1$. All the tubes are encountered for $0 \le \theta < \pi/3$; in fact, for the $\mathcal{Z}$ and the $\mathcal{A}$ nanotubes θ equals 0 and $\pi/6$, respectively, and between these chiralities lay chiral vectors of all the $\mathcal{C}$ nanotubes with $n_1 > n_2 > 0$ (the tubes (n_2, n_1), with $\pi/6 < \theta < \pi/3$, are their optical isomers).

There are $n = \mathrm{GCD}(n_1, n_2)$ (the greatest common divisor) honeycomb lattice points laying on the chiral vector. The translations for $s\vec{c}/n$ in the chiral direction, on the tube appear as the rotations for $2s\pi/n$ ($s = 0, 1, \ldots$) around the tube axis. Thus, the principal axis of order n

is a subgroup of the full symmetry of the tube (n_1, n_2):

$$\mathbf{C}_n, \quad n = \mathrm{GCD}(n_1, n_2). \tag{2}$$

Obviously, $n = n_1$ for the $\mathcal{Z}$ $(n_1, 0)$ and the $\mathcal{A}$ (n_1, n_1) nanotubes.

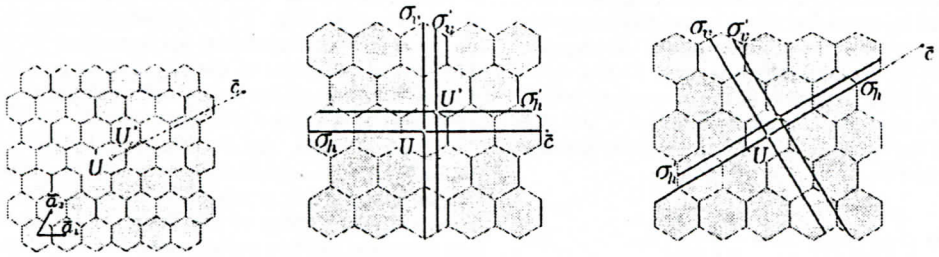

FIG. 1: **Symmetries of the honeycomb lattice.** *For the $\mathcal{C}$ $(8,6)$, $\mathcal{Z}$ $(6,0)$ and $\mathcal{A}$ $(6,6)$ tubes the chiral vectors $\vec{c}$ are depicted by the arrows. The U and U' axes pass through the circles (perpendicular to the honeycomb). In the $\mathcal{Z}$ and $\mathcal{A}$ case, the bold lines σ_v and σ_v' represent the vertical mirror and glide planes of the lattice, being orthogonal to $\vec{c}$; the planes parallel to $\vec{c}$ are denoted as σ_h and σ_h'; U is the intersection of the mirror planes, and U' of the glide planes.*

To the primitive translation of the tube corresponds the vector $\vec{a} = a_1\vec{a}_1 + a_2\vec{a}_2$ in the honeycomb lattice, being the minimal one among the lattice vectors orthogonal to $\vec{c}$. Therefore, a_1 and a_2 are coprimes, yielding

$$\vec{a} = -\frac{2n_2 + n_1}{n\mathcal{R}}\vec{a}_1 + \frac{2n_1 + n_2}{n\mathcal{R}}\vec{a}_2, \tag{3a}$$

$$a = |\vec{a}| = \frac{\sqrt{3(n_1^2 + n_2^2 + n_1 n_2)}}{n\mathcal{R}}a_0, \tag{3b}$$

with $\mathcal{R} = 3$ if $(n_1 - n_2)/3n$ is integer and $\mathcal{R} = 1$ otherwise. For the $\mathcal{Z}$ and the $\mathcal{A}$ tubes $a = \sqrt{3}a_0$ and $a = a_0$, respectively. The elementary cell of the tube is the cylinder of the height a and area $S_t = a|\vec{c}|$; it contains $S_t/S_g = 2(n_1^2+n_2^2+n_1n_2)/n\mathcal{R}$ elementary graphene cells[8]. So, the translational group $\mathbf{T}$ of the nanotube is composed of the elements $(I|ta)$, $t = 0, \pm 1, \ldots$

The encountered symmetries $\mathbf{T}$ and $\mathbf{C}_n$ originate from the honeycomb lattice translations: on the folded lattice the translations along the chiral vector become pure rotations, whereas those along $\vec{a}$ remain pure translations. These elements generate the whole nanotube from the sector of angle $2\pi/n$ of the elementary cell, with $2(n_1^2 + n_2^2 + n_1n_2)/n^2\mathcal{R}$ elementary graphene cells. This number is always greater then 1, pointing out that not all of the honeycomb lattice translations are taken into account. The missing translations are neither parallel with nor orthogonal to $\vec{c}$; on the rolled up sheet they are manifested as rotations (for the fraction of $2\pi/n$) combined with translations (for the fractions of a), yielding the screw axis of the nanotube. Their generator $(C_q^r|\frac{n}{q}a)$ corresponds to the vector $\vec{z} = r\frac{\vec{c}}{q} + n\frac{\vec{a}}{q}$ of the honeycomb lattice, which, together with the encountered translations, generates the whole honeycomb lattice. Thus, $\vec{z}$ can be chosen to form the elementary honeycomb cell together with the minimal lattice vector $\vec{c}/n$ along the chiral direction. The honeycomb cell area S_g must be the product of $|\vec{c}|/n$ and the length na/q of the projection of $\vec{z}$ onto $\vec{a}$: $a|\vec{c}|/q = \sqrt{3}a_0^2/2$. This gives the order q of the screw axis. Finally, r is found from the condition that the projections of $\vec{z}$ on $\vec{a}_1$ and $\vec{a}_2$ are coprimes. This completely determines the screw axis:

$$\mathbf{Z} = \mathbf{T}_q^r, \qquad q = 2\frac{n_1^2 + n_1n_2 + n_2^2}{n\mathcal{R}}, \tag{4a}$$

$$r = \frac{q}{n}\mathrm{Fr}\left[\frac{n(n_1 + 2n_2)}{q\mathcal{R}n_1} + \frac{n}{n_1}\left(\frac{n_1 - n_2}{n}\right)^{\varphi(\frac{n_1}{n})-1}\right], \tag{4b}$$

where $\mathrm{Fr}[x] = x - [x]$ is the fractional part of the rational number x, and $\varphi(m)$ is the Euler function, giving the number of coprimes less then m. In particular, for both the $\mathcal{Z}$ $(n,0)$ and the $\mathcal{A}$ (n,n) tubes $q = 2n$ and $r = 1$, i.e. $\mathbf{Z} = \mathbf{T}_{2n}^1$. Note that q is an even multiple of n. It is equal to the number of graphene cells in the elementary cell of the tube S_t/S_g. Therefore, q/n, the number of graphene cells in a sector, is always greater than 1; this means that all the single-wall tubes have nonsymorphic symmetry groups.

To summarize, the translational symmetry of the honeycomb lattice appears as the first family subgroup

$$\mathbf{L}^{(1)} = \mathbf{T}_q^r\mathbf{C}_n = \mathbf{L}q_p, \tag{5a}$$

$$p = q\mathrm{Fr}\left[\frac{n\mathcal{R}}{q}\frac{(\frac{2n_2+n_1}{n\mathcal{R}})^{\varphi(\frac{2n_1+n_2}{n\mathcal{R}})-1}q - n_2}{2n_1 + n_2}\right] \tag{5b}$$

of symmetries of the nanotube, with q and r given by (4). Its elements $(C_q^{rt}C_n^s|t\frac{n}{q}a)$ $(t = 0, \pm 1, \ldots, s = 0, \ldots, n-1)$

generate the whole nanotube from any adjacent pair of nanotube atoms. The group $\mathbf{L}^{(1)}$ contains all the symmetries previously considered in the literature[5,7,8,4]. Note that the screw axis used here is somewhat different frow the previously reported ones, due to the convention[16]. With this convention $2\pi/q$ is the minimal rotation in the group (followed by some fractional translation), providing that q is the order of the principle axis of the isogonal point group. This explains why q is equal to the number of graphene cells contained in the elementary cell of the tube. Note that the translational period a and the diameter D of the tube are determined by the symmetry parameters q and n:

$$a = \sqrt{\frac{3q}{2\mathcal{R}n}}a_0, \quad D = \frac{1}{\pi}\sqrt{\frac{\mathcal{R}nq}{2}}a_0. \tag{6}$$

Besides the translations, there are other symmetries of the honeycomb lattice: (a) perpendicular rotational axes through the centers of the hexagons (of order six), through the carbon atoms (of order three) and through the centers of the edges of the hexagons (of order two); (b) six vertical mirror planes through the centers of the hexagons formed by the atoms (or through the atoms); (c) two types of vertical glide planes — connecting the midpoints of the adjacent edges, and the midpoints of the next to nearest neighboring edges of the hexagons.

Among the rotations, only those for π, leaving invariant the axis of $\vec{a}$, i.e. the z-axis of the tube, remain the symmetries of the rolled-up lattice. Thus, two types of horizontal second order axes emerge as symmetries of any nanotube (Fig. 1): U, passing through the center of the deformed nanotube hexagons, and U', passing through the midpoints of the adjacent atoms. The first of these transformations is obtained when the second one is followed by the screw axis generator: $U = (C_q^r|\frac{n}{q}a)U'$. Thus, any of them, say U, complements the principle tube axis $\mathbf{C}_n$ to the dihedral point group $\mathbf{D}_n$. This shows that at least the line group $\mathbf{T}_q^r\mathbf{D}_n$ (from the 5th family) is the symmetry group of any nanotube. Note that U' just permutes the two carbon atoms in the elementary honeycomb cell, meaning that all the honeycomb atoms are obtained from an arbitrary one by the translations and the rotation U'. Analogously, the elements of the group $\mathbf{T}_q^r\mathbf{D}_n$ generate the whole nanotube from any of its atoms. The action (1) of the group elements on the point $\mathbf{r}_{000} = (\rho_0, \phi_0, z_0)$ (cylindrical coordinates) gives the points

$$\mathbf{r}_{tsu} = (C_q^{rt}C_n^sU^u|t\frac{n}{q}a)\mathbf{r}_{000} = (\rho_0, (-1)^u\varphi_0 + 2\pi(\frac{t}{q}+\frac{s}{n}), (-1)^u z_0 + t\frac{n}{q}a), \tag{7}$$

($u = 0, 1$; $s = 0, \ldots, n-1$; $t = 0, \pm 1, \ldots$); hereafter, the x-axis is assumed to coincide with the U-axis. Using (6), it can be shown that the coordinates of the first atom (positioned at $\frac{1}{3}(\vec{a}_1 + \vec{a}_2)$ on the honeycomb) are

$$\mathbf{r}_{000}^{\mathcal{C}} = (\frac{D}{2}, 2\pi\frac{n_1+n_2}{nq\mathcal{R}}, \frac{n_1-n_2}{\sqrt{6nq\mathcal{R}}}a_0). \tag{8}$$

Substituting these values in (7), the coordinates of all other atoms are obtained.

Rolling-up deforms any plane perpendicular to the graphene sheet, unless it is either parallel with $\vec{c}$ (then it becomes the horizontal plane) or orthogonal onto $\vec{c}$ (giving the vertical plane). Thus, only the tubes with the chiral vectors being parallel or orthogonal to the enumerated mirror and glide planes possess additional symmetries of these types. The $\mathcal{Z}$ and $\mathcal{A}$ tubes are immediately singled out by simple inspection. Precisely, only in these cases the chiral vector is in a perpendicular mirror plane; when the sheet is rolled up, this plane becomes the horizontal mirror plane σ_h of the corresponding nanotubes. Enlarging the previously found point symmetry group $\mathbf{D}_n$ by σ_h, the point group $\mathbf{D}_{nh}$ of the $\mathcal{Z}$ and $\mathcal{A}$ tubes is obtained. Finally, taking into account the generalized translations (4), the full symmetry groups of the single-wall nanotubes are:

$$\mathbf{L}_{\mathcal{C}} = \mathbf{T}_q^r\mathbf{D}_n = \mathbf{L}q_p22, \quad P_I = \mathbf{D}_q, \tag{9}$$

$$\mathbf{L}_{\mathcal{ZA}} = \mathbf{T}_{2n}^1\mathbf{D}_{nh} = \mathbf{L}2n_n/mcm, \quad \mathbf{D}_{2nh}. \tag{10}$$

The line group $\mathbf{T}_{2n}^1\mathbf{D}_{nh}$ (13th family) contains various new symmetries (Fig. 2), which are the combinations of the ones mentioned above. In fact, when σ_h is added to the group $\mathbf{T}_{2n}^1\mathbf{D}_n$, the other mirror and glide planes parallel or orthogonal to $\vec{c}$ are automatically included in the symmetry groups of the $\mathcal{Z}$ and $\mathcal{A}$ nanotubes. These transformations can be seen as σ_h followed by some of the elements from $\mathbf{T}_{2n}^1\mathbf{D}_n$. At first, there are n vertical mirror planes (one of them is $\sigma_v = \sigma_hU$, and the others are obtained by pure rotations; by the previous convention, the σ_h plane is the xy-coordinate plane). Also, there are the glide planes bisecting the mirror planes (e.g. the product $(\sigma_v'|\frac{1}{2}) = (C_{2n}|\frac{1}{2}a)\sigma_v$), and the vertical rotoreflection axis of order $2n$ (generated by $\sigma_vU' = C_{2n}\sigma_h'$, the reflection in the σ_h' plane, followed by the rotation for π/n).

The vectors obtained from $\vec{c}$ by the rotations from the point symmetry group $\mathbf{C}_{6v}$ of the honeycomb lattice, produce nanotubes which are essentially the same, only viewed from the rotated coordinate systems. Nevertheless, the vertical mirror plane image of $\vec{c}$ (e.g. in the vertical plane bisecting the angle of $\vec{a}_1$ and $\vec{a}_2$) produces the tube which can be considered as the same only in the

coordinate system with the opposite sign (the coordinate transformation involves the spatial inversion). Thus, the tubes (n_1, n_2) and (n_2, n_1) are the optical isomers. Only the mirror image of $\mathcal{Z}$ and $\mathcal{A}$ tube is equivalent to the original, and these tubes have no optical isomers[10]. Concerning the symmetry groups, if $\mathrm{T}_q^r\mathrm{C}_n$ corresponds to the tube (n_1, n_2), then the group of the tube (n_2, n_1) is $\mathrm{T}_q^{\frac{s}{q}-r}\mathrm{C}_n$ (although isomorphic, these groups are equal only when $q = 2n$ and $r = 1$, i.e. only for the $\mathcal{Z}$ and the $\mathcal{A}$ tubes).

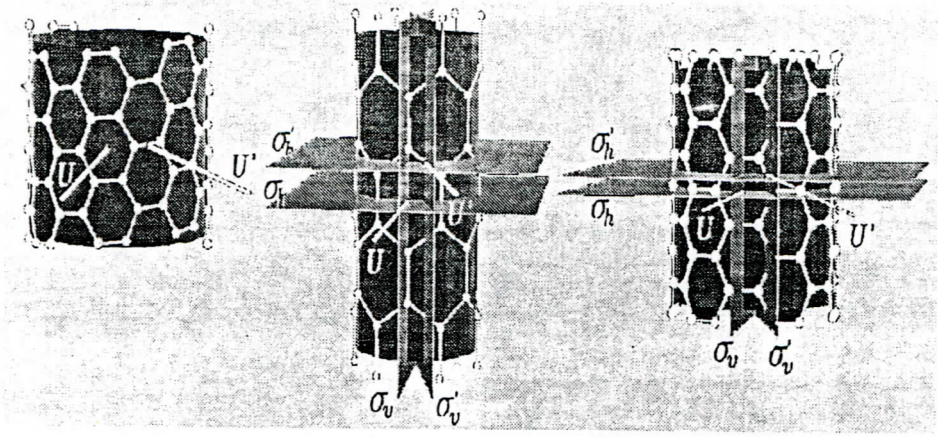

FIG. 2: **Symmetries of the single-wall nanotubes:** (8,6), (6,0) *and* (6,6). *The horizontal rotational axes U and U' are symmetries of all the tubes, while the mirror planes (σ_v and σ_h), the glide plane σ_v' and the rotoreflection plane σ_h' are symmetries of the $\mathcal{Z}$ and $\mathcal{A}$ tubes only. The line groups are* $\mathrm{T}_{148}^{21}\mathrm{D}_2$ *for (8,6), and* $\mathrm{T}_{12}^{1}\mathrm{D}_{6h}$ *for the other two tubes.*

B Single-wall tubes with different elements

After the discovery of carbon nanotubes, their predicted and partly experimentally observed diverse properties attracted much interest. This induced (from 1994) attempts to synthesize and investigate some other similar structures. All these studies are based on the honeycomb like lattices. Thus, the compounds with more or less stable hexagonal layered phase attracted attention: boron and nitrite, together with the carbon atoms immediately appeared as the candidates. Thus, several tubes of this type, commonly denoted by $\mathrm{B_xC_yN_z}$ were observed and roughly theoretically considered: BN, $\mathrm{BC_3}$, $\mathrm{BC_2N}$ (two modifications). Here we consider symmetry groups of these single wall tubes. They are derived with help of the known line group of SWCT. Recently, quite different types of the $\mathrm{MoS_2}$ and $\mathrm{WS_2}$ tubes are synthesized[17].

1 BN tubes

As it can be seen from the Figure 4, the main difference of these tubes[18,19] compared to SWCT is that U axis is absent. Therefore, the whole tube is the two orbit system of the index two subgroups of (9) and (10):

$$\mathrm{L}_{\mathcal{C}} = \mathrm{T}_q^r\mathrm{C}_n = \mathrm{L}q_p, \quad P_I = \mathrm{C}_q, \tag{11}$$

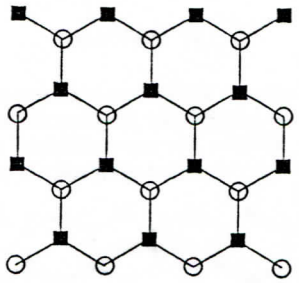

FIG. 3: **Hexagonal lattice of BN** (B= ○, N= ■).

with p, q, r and n same as in (9), and

$$\mathrm{L}_{\mathcal{Z}} = \mathrm{T}_{2n}^1\mathrm{C}_{nv} = \mathrm{L}2n_n mc, \quad P_I = \mathrm{C}_{2nv}. \tag{12}$$
$$\mathrm{L}_{\mathcal{A}} = \mathrm{T}_{2n}^1\mathrm{C}_{nh} = \mathrm{L}2n_n/m, \quad P_I = \mathrm{C}_{2nh}. \tag{13}$$

2 BC_3 tubes

Their symmetry groups are the same as those of SWCT, but the unit length is doubled, since the translational periods[20,18] of the lattice are $\vec{A}_i = 2\vec{a}_i$ (i =

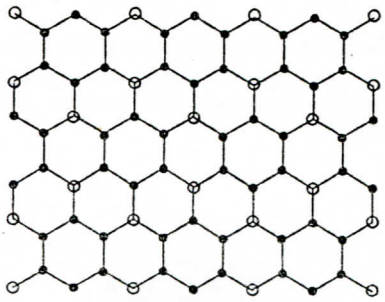

FIG. 4: Lattice BC_3 (B= ∘, C=•).

1,2), and the BC_3 tube (n_1, n_2) has the chiral vector $n_1\vec{A}_1 + n_2\vec{A}_2$. The unit cell contains four honeycomb cells, figure 4. Such cells make the same honeycomb lattice as graphene, with the same symmetry elements and the complete derivation of various expressions as for the SWCT, except that the new periods $\vec{A}_i$ are to be used instead of $\vec{a}_i$. For $\mathcal{C}$ tubes there are three C-orbits and one B-orbit, while in the case of $\mathcal{Z}$ and $\mathcal{A}$ tubes, only one B and two C-orbits are present; in fact, since C atoms are not in the completely special positions as in SWCT, the mirror planes leave only one of the carbon $L_{\mathcal{C}}$ orbits invariant, while the remaining two become a single orbit of $L_{\mathcal{ZA}}$.

3 BC_2N tubes

There are several 2D lattices with this chemical structure. Here we consider only the two most stable[21,18] configurations. Despite the same chemical contents, their geometry and the resulting symmetry is quite different.

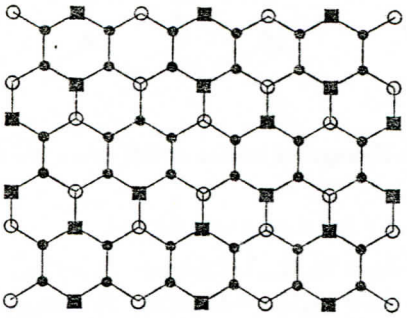

FIG. 5: Type 1 lattice of BC_2N.

The first type (Fig. 6) can be considered like the BC_3 tube, with the periods $\vec{A}_i$, i.e. with the same groups as SWCT, but with the doubled unit length. Nevertheless, only $C_6^3 = U$ rotation and two vertical mirror planes are the symmetries of the lattice. Although exactly these yield the symmetries of the tube (thus the tube groups are not changed), the absence of the remaining elements means that the inequivalent tubes are contained between the chiral angles 0 and $\pi/2$. These two limiting directions $(n, 0)$ and $(-n, 2n)$ define the $\mathcal{Z}$ and $\mathcal{A}$ tubes respectively, all the remaining ones being the $\mathcal{C}$ tubes. The $\mathcal{C}$ tubes contain two C, one B and one N orbits; C orbits are joined in the single C orbit of $\mathcal{Z}$ and $\mathcal{A}$ tubes.

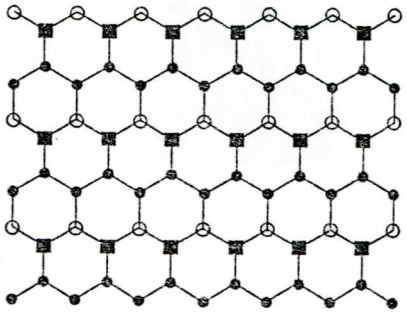

FIG. 6: Type 2 lattice of BC_2N.

The second type of the BC_2N tubes has the underlying lattice presented in Fig. 6. Obviously the elementary cell is doubled with respect to the graphite, with the translational periods being $\vec{a}_1$ and $\vec{A}_2 = 2\vec{a}_2$. There are no rotational symmetries of the 2D lattice, but the vertical mirror plane σ_x enables to consider as inequivalent tubes (optical isomers are assumed equivalent) only those with the chiral angles between 0 and $\pi/2$; again, the tubes with $\theta = 0$ are $\mathcal{Z}$, these with $\theta = \pi/2$ are $\mathcal{A}$ and the others are $\mathcal{C}$ tubes. The tube $(n1, n2)$ has the chiral vectors $n_1\vec{a}_1 + 2n_2\vec{a}_2$, i.e. it corresponds to SWCT $(n_1, 2n_2)$. Nevertheless, their symmetry groups are different, since no U-axis and no translations with an odd $\vec{A}_2$-component remain in the BC_2N tube symmetry group. Thus only the halving subgroup of the first family subgroup (5) of the corresponding $(n_1, 2n_2)$ SWCT is the final symmetry group in the $\mathcal{C}$ case (of course, all the parameters q, r, n, p etc. are given by the corresponding SWCT expressions with n_2 substituted by $2n_2$). It can be shown[22] that this halving subgroup is:

$$L_{\mathcal{C}} = \begin{cases} \text{if } n_2/n \text{ even:} \\ T_{q/2}^{r\ (\mathrm{mod}\ q/2)} C_n = L(q/2)_{p\ (\mathrm{mod}\ q/2)},\ A = a \\ \text{if } n_2/n \text{ odd and } \begin{matrix}\mathcal{R}=1 \text{ and } n_1/n \text{ even, or} \\ \mathcal{R}=3 \text{ and } n_1/n \text{ odd}\end{matrix}, \\ T_q^{((p+q)/n)^{-1}\ (\mathrm{mod}\ 2q/n)} C_{n/2} = L_{q(p+q)/2},\ A = 2a \\ \text{if } n_2/n \text{ odd and } \begin{matrix}\mathcal{R}=3 \text{ and } n_1/n \text{ even, or} \\ \mathcal{R}=1 \text{ and } n_1/n \text{ odd}\end{matrix}; \\ T_q^{(p/n)^{-1}\ (\mathrm{mod}\ 2q/n)} C_{n/2} = L_{qp/2},\ A = 2a \end{cases} \tag{14}$$

the resulting translational period A is also given, while $\mathcal{R}$, q, n, r and a correspond to SWCT $(n_1, 2n_2)$. For the achiral tubes these halving subgroups reduce to the symorphic groups, which are to be completed by σ_v for $\mathcal{Z}$, and σ_h for $\mathcal{A}$ tubes. The $\mathcal{Z}$ tubes satisfy the first condition, and the addition of σ_v gives:

$$\mathrm{L}_{\mathcal{Z}} = \mathrm{TC}_{nv} = \mathrm{L}nmm, \mathrm{L}nm \quad A = a. \qquad (15)$$

Analogously, in the $\mathcal{A}$ case $(-n, n)$ the first possibility of (14) is realized; together with the horizontal mirror plane this gives

$$\mathrm{L}_{\mathcal{A}} = \mathrm{TC}_{n\bar{h}} = \mathrm{L}(\overline{2n}), \mathrm{L}n/m, \quad A = a. \qquad (16)$$

Note that the tubes $(2n, n)$, corresponding to $\mathcal{A}$ SWCT, satisfy the second condition of (14), with the group $\mathrm{L}_C = \mathrm{T}^3_{1n}\mathrm{C}_n = \mathrm{L}q_3$. There are two C orbits, one B orbit and one N orbit independently of the chiral vector.

C Double- and multi-wall nanotubes

The symmetry of a multi-wall nanotube can be found now as the intersection of the symmetry groups of its single-wall constituents. This task will be considered for the double-wall tubes at first, and then the results are straightforwardly generalized to the multi-wall ones. The intersection of the line groups, $\mathrm{L} = \mathrm{ZP}$ and $\mathrm{L}' = \mathrm{Z}'\mathrm{P}'$ has the form $\mathrm{L}_2 = \mathrm{Z}_2(\mathrm{P} \cap \mathrm{P}')$. Thus, the intersection of the point groups is looked for independently of the generalized translations.

As it has been derived in (2), the tubes (n_1, n_2) and (n_1', n_2') are invariant under the rotations around their axes for the multiples of angles $2\pi/n$ and $2\pi/n'$ ($n = \mathrm{GCD}(n_1, n_2)$, $n' = \mathrm{GCD}(n_1', n_2')$), respectively. The tube composed of these coaxially arranged components is invariant under the rotation for $2\pi/N$, which is the minimal common rotation of the components, and its multiples. Thus, the principle axis subgroup of the double-wall nanotube is C_N, with $N = \mathrm{GCD}(n, n') = \mathrm{GCD}(n_1, n_2, n_1', n_2')$. The horizontal second order rotational axis U (and U') is also the symmetry of all single-wall nanotubes. Nevertheless, such an axis remains the symmetry of the composite tube only if it is common to all of the components, and then the point symmetry is D_N. Obviously, if a nanotube contains at least one chiral component, then D_N is its maximal point symmetry. Only the tubes composed exclusively of the $\mathcal{Z}$ and $\mathcal{A}$ single-wall components may have additional mirror and glide planes, as well as the rotoreflectional axis. Analogously to the horizontal axis, these are the symmetries of the whole tube only if they are common to all of the components (the rotoreflectional axis appears only if the horizontal planes σ_h' coincide).

After the point symmetries are completely determined, there remauns the more difficult study of the generalized translational factor Z_2. At first, note that it may be completely absent. Suppose that a double-wall tube has the translational period A. If the translational periods of its constituents are a and a', then A is obviously the minimal distance being a multiple both of a and of a': $A = \alpha a = \alpha' a'$, where α and α' are positive coprimes (to assure minimality). Thus, the double-wall tube is translationally periodic if and only if the translational periods of its constituents are commensurate, i.e. only when a'/a is rational. On the contrary, if a'/a is an irrational number, the composed tube is not translationally periodic, and Z_2 is trivial (identical transformation only); the total symmetry reduces to the already found point group.

In the commensurate case it remains to examine if the translational group can be refined by a screw axis, common to all of the single-wall components. The task is to determine the screw axis generator $(C_Q^R|F)$ with maximal Q, appearing in the both groups $\mathrm{L} = \mathrm{T}^r_q\mathrm{C}_n$ and $\mathrm{L}' = \mathrm{T}^{r'}_{q'}\mathrm{C}_{n'}$. Thus, one is looking for the values of Q, R and F (in accordance with the convention[16]), such that there exist integers t, s, t' and s' (enumerating the elements of L and L') satisfying

$$(C_Q^R|F) = (C_q^{rt}C_n^s|tf) = (C_{q'}^{r't'}C_{n'}^{s'}|t'f') \qquad (17)$$

with $F = \frac{N}{Q}A$, $f = \frac{n}{q}a$, and $f' = \frac{n'}{q'}a'$. Obviously, the

TABLE II: **Symmetry of the multi-wall $\mathcal{Z}$ and $\mathcal{A}$ carbon tubes.** *For the periodic tubes, the line groups (and families) and the isogonal groups are in the "odd" columns if all the ratios n/N, n'/N, ... are odd, and in the "even" columns otherwise. The point groups of the tubes with both $\mathcal{Z}$ and $\mathcal{A}$ components is in the last column. In the first column the relative positions of the component tubes are characterized by the coinciding symmetry elements (beside the common principle axis in the general position). Here, (U, U') denotes the horizontal axis, which is U-axis in some of the constituents, and U'-axis in the remaining ones (to exclude the additional mirror or glide planes). Also, (σ_h, σ_h') is the plane being σ_h in some of constituents (with even n, necessarily), and σ_h' in the remaining tubes; in the incommensurate case, the same groups are obtained when σ_h' planes are in common.*

Relative position	Line group "Odd"		Line group "Even"		Isogonal group "Odd"	Isogonal group "Even"	PG
General	$\mathrm{T}^1_{2N}\mathrm{C}_N$	(1)	TC_N	(1)	C_{2N}	C_N	C_N
σ_h	$\mathrm{T}^1_{2N}\mathrm{C}_{Nh}$	(4)	TC_{Nh}	(3)	C_{2Nh}	C_{Nh}	C_{Nh}
σ_v	$\mathrm{T}^1_{2N}\mathrm{C}_{Nv}$	(8)	TC_{Nv}	(6)	C_{2Nv}	C_{Nv}	C_{Nv}
σ_v'	$\mathrm{T}^1_{2N}\mathrm{C}_{Nv}$	(8)	$\mathrm{T}_c\mathrm{C}_{Nv}$	(7)	C_{2Nv}	C_{Nv}	C_N
(U, U')	$\mathrm{T}^1_{2N}\mathrm{D}_N$	(5)	TD_N	(5)	D_{2N}	D_N	D_N
σ_h, σ_v	$\mathrm{T}^1_{2N}\mathrm{D}_{Nh}$	(13)	TD_{Nh}	(11)	D_{2Nh}	D_{Nh}	D_{Nh}
σ_h, σ_v'	$\mathrm{T}^1_{2N}\mathrm{D}_{Nh}$	(13)	$\mathrm{T}_c\mathrm{C}_{Nh}$	(12)	D_{2Nh}	D_{Nh}	C_{Nh}
(σ_h, σ_h')	$\mathrm{T}^1_{2N}\mathrm{C}_{Nh}$	(4)	TS_{2N}	(2)	C_{2Nh}	S_{2N}	S_{2N}
$(\sigma_h, \sigma_h'), \sigma_v$	$\mathrm{T}^1_{2N}\mathrm{D}_{Nh}$	(13)	TD_{Nd}	(9)	D_{2Nh}	D_{Nd}	D_{Nd}
$(\sigma_h, \sigma_h'), \sigma_v'$	$\mathrm{T}^1_{2N}\mathrm{D}_{Nh}$	(13)	$\mathrm{T}_c\mathrm{S}_{2N}$	(10)	D_{2Nh}	D_{Nd}	S_{2N}

fractional translation F is the multiple $F = tF^*$ of the minimal common fractional translation F^*, implying $A = \frac{Q}{N}tF^*$. Analogously to A, the translation F^* is found as the minimal distance being the multiple both of f and f'; thus it is given by the unique solution in the coprimes ϕ and ϕ' of the equation $F^* = \phi f = \phi' f'$. Since the translational periods of the single-wall components are multiples of their fractional translations, A is the multiple of F^*, i.e. $A = \Phi F^*$. With the help of number theory, it can be shown that only the tubes with the same $\mathcal{R}$ may be commensurate; then $\alpha = \phi' = \sqrt{\frac{q'/n'}{\mathrm{GCD}(q/n, q'/n')}}$, $\alpha' = \phi = \sqrt{\frac{q/n}{\mathrm{GCD}(q/n, q'/n')}}$ and $\Phi = \sqrt{\frac{qq'}{nn'}}$. Thus, $Q = \Phi N/\tau$, and the minimal τ is looked for to provide the finest screw axis. The translational part of (17) immediately shows that $t = \tau\alpha'$ and $t' = \tau\alpha$. With these values substituted, the rotational part of (17) gives:

$$C_Q^R = C_q^{r\alpha'\tau} C_n^s = C_{q'}^{r'\alpha\tau} C_{n'}^{s'}. \tag{18}$$

The minimal τ for which this equation is solvable in s and s' is $\tau = \Phi/\mathrm{GCD}(r\alpha\frac{n'}{N} - r'\alpha'\frac{n}{N}, \Phi)$. Finally, $Q = N\mathrm{GCD}(r\alpha\frac{n'}{N} - r'\alpha'\frac{n}{N}, \sqrt{\frac{qq'}{nn'}})$, and R is easily found from the first equation (18).

All these results are immediately generalized to the multi-wall tubes. Note that the generalized translations and the principle rotational axis of the multi-wall nanotube depend only on the types of their single-wall components. On the contrary, the appearance of the mirror and glide planes and the horizontal axes in the common symmetry group is additionally determined by the relative positions of these components.

It remains to give the summary of the symmetry groups of the multi-wall tubes. If at least one of the single-wall constituents is chiral, then in the commensurate case there are two possibilities: $\mathbf{T}_Q^R\mathbf{C}_N$, corresponding to the general mutual position, and $\mathbf{T}_Q^R\mathbf{D}_N$ in the special mutual positions with the common U-axis. Analogously, the tube built of the incommensurate components have the symmetry described by the point groups $\mathbf{C}_N$ or $\mathbf{D}_N$. If the nanotube is built of the $\mathcal{Z}$ and $\mathcal{A}$ single-wall tubes $(n,0)$ (or (n,n)), $(n',0)$ (or (n',n')), ..., the order of the principle rotational axis is $N = \mathrm{GCD}(n, n', \ldots)$. If the tube contains at least one single-wall tube of both types, no translational periodicity appears and its symmetry is described by the point group (Tab. II). On the other hand, for the tube composed of the components of the same type (either $\mathcal{Z}$ or $\mathcal{A}$), the translation period is equal to that of the components. Two different situations may occur: if all the integers n/N, n'/N ... are odd ("odd" case), the translations are refined by the screw axis $\mathbf{T}_{2N}^1$; otherwise, if at least one of these integers is even ("even" case), no screw axis emerges. The analysis of the special arrangements of the constituents with common horizontal axes, mirror or glide planes, increasing the symmetry of the total system is summarized in Table II. Note that according to the various arrangements of the components, any of the line and axial point groups may be the resulting symmetry for the commensurate and incommensurate components, respectively. Some examples are given in the next section.

IV. POTENTIALS IN NANOTUBES

Potentials produced by the single-wall nanotube must be invariant under the transformations of its symmetry group $\mathbf{L}$. This means that the potential $V(\mathbf{r})$ is a spatial function obeying

$$V(\mathbf{r}) = V((P|t)^{-1}\mathbf{r}), \tag{19}$$

for each element $(P|t)$ of $\mathbf{L}$ acting according to (1). In the forthcoming analysis this property is used to obtain quite restrictive conditions on the form of V. Since the invariance under the generators implies the invariance under the whole group, the relation (19) should be inspected only for the generators of $\mathbf{L}$, to find the independent conditions. The single-wall nanotubes will be treated explicitly, but hints for generalization to the multi-wall ones will be given, too.

The translational and rotational symmetries of the tube, generated by $(I|a)$ and C_n, immediately enable one to get the Fourier expansion in the cylindrical coordinates φ and z:

$$V(\mathbf{r}) = \sum_{K,M=-\infty}^{\infty} \alpha_K^M(\rho) e^{inM\varphi} e^{i\frac{2\pi}{a}Kz}. \tag{20}$$

To incorporate the whole subgroup $\mathbf{L}^{(1)}$, the screw axis generator $(C_q^r|\frac{n}{q}a)$ should be employed. The relation (19) becomes $V(\rho,\varphi,z) = V(\rho, \varphi - \frac{2\pi}{q}r, z - \frac{n}{q}a)$. When applied to (20), this helical group restricts the sum only to the terms with $Mr + K$ being the multiple of q/n:

$$V(\mathbf{r}) = \sum_{\substack{K,M=-\infty \\ Mr=-K \bmod(\frac{q}{n})}}^{\infty} \alpha_K^M(\rho) e^{inM\varphi} e^{i\frac{2\pi}{a}Kz}. \tag{21}$$

For the $\mathcal{Z}$ and the $\mathcal{A}$ tubes $q = 2n$ and $r = 1$, and the restriction $M = -K \bmod(2)$ reduces the sum to the terms with K and M of the same parity:

$$V(\mathbf{r}) = \sum_{\substack{M,K=-\infty \\ \text{odd}}}^{\infty} \omega_K^M(\rho) e^{iMn\varphi} e^{iK\frac{2\pi}{a}z} + \sum_{\substack{M,K=-\infty \\ \text{even}}}^{\infty} \epsilon_K^M(\rho) e^{iMn\varphi} e^{iK\frac{2\pi}{a}z}. \tag{22}$$

Additional symmetries are manifested as relations between the coefficients $\alpha_K^M(\rho)$ in (21). The invariance under the horizontal U-axis reads $V(\rho,\varphi,z) = V(\rho,-\varphi,-z)$, giving $\alpha_K^M(\rho) = \alpha_{-K}^{-M}(\rho)$; thus, the most general potential of the $\mathcal{C}$ single-wall nanotube is:

$$V(\mathbf{r}) = \sum_{\substack{K,M=0 \\ Mr=-K \bmod(\frac{q}{n})}}^{\infty} \pi_K^M(\rho)\cos(\frac{2\pi}{a}Kz + nM\varphi) + \sum_{\substack{K,M=0 \\ Mr=K \bmod(\frac{q}{n})}}^{\infty} \mu_K^M(\rho)\cos(\frac{2\pi}{a}Kz - nM\varphi). \tag{23}$$

As for the $\mathcal{Z}$ and $\mathcal{A}$ tubes, the potential (22) is invariant under σ_v and U. For further purposes σ_v is considered first: manifesting as the requirement $V(\rho,\varphi,z) = V(\rho,-\varphi,z)$, it gives $\omega_K^M = \omega_K^{-M}$ and $\epsilon_K^M = \epsilon_K^{-M}$, and the potential (the most general one for the line group $\mathbf{T}_{2n}^1\mathbf{C}_{nv}$, of the 8th family) becomes:

$$V(\mathbf{r}) = \sum_{\substack{K=-\infty \\ \text{odd}}}^{\infty}\sum_{M=1\text{odd}}^{\infty} \omega_K^M(\rho)\cos(Mn\varphi)e^{iK\frac{2\pi}{a}z} + \sum_{\substack{K=-\infty \\ \text{even}}}^{\infty}\sum_{\substack{M=0 \\ \text{even}}}^{\infty} \epsilon_K^M(\rho)\cos(Mn\varphi)e^{iK\frac{2\pi}{a}z}. \tag{24}$$

Including U-axis as in (23), the general $\mathcal{Z}$ and $\mathcal{A}$ potential is obtained:

$$V(\mathbf{r}) = \sum_{\substack{M,K=1 \\ \text{odd}}}^{\infty} \omega_K^M(\rho)\cos(\frac{2\pi}{a}Kz)\cos(Mn\varphi) + \sum_{\substack{M,K=0 \\ \text{even}}}^{\infty} \epsilon_K^M(\rho)\cos(\frac{2\pi}{a}Kz)\cos(Mn\varphi). \tag{25}$$

Note that due to the implicitly encountered σ_h invariance, all the terms are invariant under the z-axis reversal, in contrast to the $\mathcal{C}$ case.

The obtained potentials can be further specified. When the Taylor expansion of $\alpha_K^M(\rho)$ is performed, the sum of the terms with the same order in ρ is invariant polynomial of the line group. Therefore, this is a polynomial over the integrity basis of the line group[23], with very restricted form. As for the translationally periodic multi-wall tubes, the method described can be applied, with analogous results. Different situation is with the nanotubes having incommensurate components. They have only point group symmetries, acting on the coordinates according to the homogeneous rules. Instead of the Fourier expansions in φ and z, the total Taylor expansion is considered, with terms being invariant polynomials in all the coordinates. So, only the Molien functions[1] and the integrity bases for the point groups are to be used[24]. These topics will be considered elsewhere in details, while in the rest of the section some important implications of the presented results will be derived. For simplicity, the $\mathcal{Z}$ and $\mathcal{A}$ nanotubes will be considered.

The separation of the even and odd terms characterizes the potentials (22), (24) and (25), related to the screw axis $\mathbf{T}_{2n}^1$ of the $\mathcal{Z}$ and $\mathcal{A}$ tubes. Beside the terms independent of z, in the even part there are the terms with the translational periods being fractions of $a/2$. The periods of the odd harmonics are odd fractions of the original period a of the tube. All the terms with the periodicity of the tube, i.e. with $K = 1$, have nontrivial rotational periodicity $\frac{2\pi}{Mn}$. Of course, this reveals the influence of the helical nature of the tube to its physical properties. For example, the constant electric field along the tube axis breaks the z-reversal symmetries, lowering the symmetry group to $\mathbf{T}_{2n}^1\mathbf{C}_{nv}$, and the caused current density is given by (24). Therefore, either the local density variations are only due to the harmonics with the periods being even fractions of $\frac{a}{2}$, or there are chiral current components; this can be experimentally tested. In fact, all the terms with $M, K \neq 0$ also give this interesting possibility.

Finally, possible relative position of the double-wall tube consisting of $\mathcal{Z}$ or $\mathcal{A}$ components will be discussed. Their mutual interaction can be considered as the sum of the potentials that the atoms of the second tube ($(n',0)$ or (n',n')) experience in the field (25) produced by the first tube $(n,0)$ or (n,n). The potential of the whole second nanotube becomes $\sum_{t=-\infty}^{\infty}\sum_{s=0}^{n'}\sum_{u=0}^{1} V(\mathbf{r}_{tsu})$. This sum depends on the relative positions of the single-wall components, which are parameterized by the angle φ_0 and the height z_0 between their U axes. With help of (7) and (8) the potential $V_n^{n'}$ over the single atom can be calculated. For $\mathcal{ZA}$ and $\mathcal{AZ}$ tubes, the obtained potential is constant, i.e. independent of the relative position of the single-wall components. This is natural consequence of the incommensurability of the $\mathcal{Z}$ and $\mathcal{A}$ tubes. Namely, two coaxial incommensurate helices pass through all the possible mutual positions, independently on their initial points (the tube is considered to be long enough), and none of their relative spatial positions is singled out. Thus, no energy is required for relative coaxial translations and rotations of the components, and this is manifested as the obtained constant potential. In the cases of $\mathcal{ZZ}$ and $\mathcal{AA}$ tubes one finds (the constants ω_K^M and ϵ_K^M are the values of the coefficients in the radius $\rho = D'/2$ of the second tube and $N = \mathrm{GCD}(n,n')$):

$$V_n^{n'} = \sum_{\substack{M,K=1 \\ \text{odd}}}^{\infty} \omega_K^M\cos(\frac{2\pi}{a}Kz_0)\cos(\frac{nn'}{N}M\varphi_0)\sin^2(\frac{\pi nn'}{2N^2}) + \sum_{\substack{M,K=1 \\ \text{even}}}^{\infty} \epsilon_K^M\cos(\frac{2\pi}{a}Kz_0)\cos(\frac{nn'}{N}M\varphi_0). \tag{26}$$

Note that the odd terms appear only in the "odd" case (Tab. II), with the symmetry group $\mathbf{T}_2^1\mathbf{C}_N$ in the general

position. The minima of this potential single out the preferred relative positions of the tubes. The importance of such analysis stems from the expected dependence of the properties of the tube on the relative positions of the components, as illustrated in the discussion of the optical activity. For further considerations some assumption on the realistic forces between the components is needed. Here, we only note that an absolute extremal point of the potential is $\varphi_0 = z_0 = 0$, i.e. the position of coincident U-axis of the components. Thus, the maximal symmetry positions are preferred if the forces are attractive.

V. CONCLUDING REMARKS

All the geometrical symmetries of the nanotubes are found. In addition to the rotations, translations and screw-axes, observed previously, the single-wall carbon tubes always possess horizontal rotational axes; the $\mathcal{Z}$ and $\mathcal{A}$ ones have mirror and glide planes in addition. Thus, their full symmetry group is $\mathrm{T}^r_q\mathrm{D}_n$ for the single-wall $\mathcal{C}$ tubes and $\mathrm{T}^1_2\mathrm{D}_{nh}$ for $\mathcal{Z}$ and $\mathcal{A}$ ones. The parameters q and r of the helical group are found in the closed form. Since $2\pi/q$ is the angle of the minimal rotation (combined with the fractional translation) performed by the symmetry group, the order of the principle axis of the isogonal group is q and it is always even. Moreover, $2q$ is the number of the carbon atoms in the elementary translational cell of the tube. Let us mention that the different tubes cannot have the same symmetry parameters q, r, n and a. This profound property means that the line group is sufficient to reconstruct the tube (as it is demonstrated by (7)), i.e. the symmetry completely determines the geometry and all consequent characteristics of the nanotube. The symmetries of the multi-wall tubes are quite diverse. Depending on the types of the single-wall components and their arrangements, all the line and axial-point groups emerge: $\mathcal{A}$ and $\mathcal{Z}$ tubes can be combined to make a prototype for any line or axial symmetry group. This immediately shows that the properties of nanotubes may vary greatly, depending not only on the single-wall constituents, but also on their mutual positions.

There are many physical properties based on symmetry, and the presented classification of nanotubes according to their symmetry can be widely exploited. At first, the symmetry can be used to find good quantum numbers. We begin with the single-wall nanotubes. The translational periodicity is reflected in the conserved quasi-momentum k, taking the values from the 1D Brillouin zone $(-\pi, \pi]$, or its irreducible domain[25] $[0, \pi]$. Also, the z-component of the quasi-angular momentum m is the quantum number caused by the symmetry of the principle rotational axis; it takes on the integer values from the interval $(-\frac{n}{2}, \frac{n}{2}]$, and characterizes the nanotube quantum states. The parity with respect to reversal of the z-axis, induced by the horizontal rotational axis U, is the last quantum number common to all the single-wall tubes. The even and the odd states with respect to this parity are conventionally denoted by $+$ and $-$. For the $\mathcal{Z}$ and $\mathcal{A}$ tubes there is an additional vertical mirror plane parity, introducing the quantum numbers A and B, to distinguish between the even and the odd states (the parity with respect to the horizontal mirror plane is dependent on the above discussed U and σ_v parities, $\pm$ and A/B). Concerning the multi-wall tubes, m is the quantum number again. Again, the z-reversal and vertical mirror parities may appear, depending on the concrete symmetry of the nanotube. Nevertheless, the tubes with incommensurate components are not periodic, and in such cases the quasi-momentum k is not an appropriate quantum number; an interesting experimental question may be whether the approach of modulated systems can be applied to restore this quantity. The simple criterion of commensurability of the single-wall tubes is derived: they have the same $\mathcal{R}$ and $\sqrt{\frac{qq'}{nn'}}$ is an integer. The involved symmetry parameters q and n are discrete, allowing exact experimental check of commensurability.

The enumerated quantum numbers may be used to discuss and predict many characteristics of the nanotubes, but the most sophisticated approach to classification and properties of different quantum states is based on the irreducible representations of the corresponding line[26,27] and point groups. Let us remind that these representations are labeled by the derived quantum numbers. The most exhaustive possible information on selection rules, comprising the conservation of quantum numbers, for the processes in the nanotubes has become available[28] after the full line (or point) group symmetry has been established.

The dimension of an irreducible representation equals the degeneracy of the corresponding energy level. For the periodic tubes, the degeneracy of the energy bands is at most fourfold; nevertheless, if the time reversal symmetry of the (spin-independent) Hamiltonian is encountered, the maximal degeneracy is eight-fold[29]. Further, the possible degeneracies are only two-, four- and eight-fold. As for the multi-wall nanotubes with incommensurate components, the dimensions of the irreducible representations of the axial point groups are one, two and (if the time reversal symmetry is included) four, showing the possible degeneracies of the energy levels. Note that the maximal of the enumerated degeneracies (eight- and four-fold) is not possible for the tubes containing at least one $\mathcal{C}$ single-wall component. Moreover, the degeneracy of the multi-wall tube in the general position of its component is at most two-fold, which is caused by the time reversal symmetry exclusively.

The results of the section IV enable us to generalize the Bloch theorem to the line group symmetries of the single-wall nanotubes[7]: multiplying these invariant functions by the matrix elements of the corresponding irreducible representation, all the quantum states and covariant functions can be obtained. On the other hand, many

of the nanotube properties can be understood on the basis of these potentials. The mutual independence of the incommensurate ideal infinite coaxial tubes is an interesting result, that should be understood as the weak coupling in the realistic cases. Relative arrangement of two coaxial single-wall tubes is sharply reflected on the tensor properties of the tubes, as illustrated by the optical activity[10]. In this context, the discussion of the preferred positions, being briefly described, should be important for applications of nanotubes, as well as the proposed possibility of the chiral currents. The fields produced by such currents could be used for tube identification.

REFERENCES

† Electronic address: yqoq@afrodita.rcub.bg.ac.yu; URL: `http://www.ff.bg.ac.yu/qmf/qsg_e.htm`

[1] M. V. Jarić and J. L. Birman, J. Math. Phys., **18**, 1456 (1977); **18**, 1459 (1977).

[2] S. Iijima, Nature, **354**, 56 (1991).

[3] M. S. Dresselhaus, *Carbon Nanotubes*, APS Tutorial, 1998.

[4] M. S. Dresselhaus, G. Dresselhaus, and P. C. Eklund, *Science of Fullerenes and Carbon Nanotubes* (Academic Press, San Diego, 1998).

[5] M. S. Dresselhaus, G. Dresselhaus, and R. Saito, Phys. Rev. B **45** 6234 (1992).

[6] N. Hamada, S. Sawada, and A. Oshiyama, Phys. Rev. Lett. **68**, 1579 (1992).

[7] C. T. White, D. H. Robertson, and J. W. Mintmire, Phys. Rev. B **47** 5485 (1993).

[8] R. A. Jishi, L. Venkataraman, M. S. Dresselhaus, and G. Dresselhaus, Phys. Rev. B, **16** 11176 (1995).

[9] M. Damnjanović, I. Milošević, T. Vuković, and R. Sredanović R, *J. Phys. A: Math. Gen.* **32**, 4097-4104 (1999).

[10] M. Damnjanović, I. Milošević, T. Vuković, and R. Sredanović R, *Phys. Rev. B* **60**, 2728-2739 (1999).

[11] I. Milošević, Phys. Lett. A **204** 63 (1995).

[12] M. Damnjanović, T. Vuković, and I. Milošević, J. Phys A: Math. Gen. (to appear).

[13] I. Milošević, R. Živanović, and M. Damnjanović, Polymer, **38** 4445 (1997).

[14] I. Milošević, A. Damjanović, and M. Damnjanović, ch. XIV in *Quantum Mechanical Simulation Methods for Studying Biological Systems*, eds. D. Bicout and M. Field (Springer-Verlag, Berlin, 1996).

[15] J. P. Elliot and P. G. Dawber, *Symmetry in Physics* (London: Macmillan, 1979)

[16] The standard notation is used: σ_v is vertical mirror plane, I is 3×3 identity matrix, while a denotes the translational period. Also, C_q^r is the rotation for $2\pi r/q$ around z-axis, where $0 \leq r < q/n$ and q/n are coprime integers. Instead of the helical group $\mathbf{Z}$, generated by $(C_q^r|\frac{n}{q}a)$, the groups generated by $(C_q^{r_i}|\frac{n}{q}a)$, with $r_i = r + i\frac{q}{n}$, $i = 1, \ldots, n-1$, give the same full symmetry group[7]. Among these r_i there is at least one being coprime with q; with this r_i, it is obvious that the set $(C_q^{tr_i}|t\frac{n}{q}a)$ contains the rotations for all the multiples of $2\pi/q$ (followed by some translations).

[17] M. Remskar, Z. Skraba, F. Cleton, R. Sanjines, and F. Levy, Surf. Rev. Lett. **5**, 423 (1998); Appl. Phys. Lett. **69**, 351 (1996); M. Remskar, Z. Skraba, M. Regula, C. Ballif, R. Sanjines, and F. Levy, Advanced Mat. **10**, 13 (1998).

[18] Z. Weng-Sieh *et al.*, Phys. Rev. B **51** 11229 (1995).

[19] A. Rubio, J. L. Korkill, and M. L. Cohen, Phys. Rev. B **49** 5081; X. Blase, A. Rubio, S. G. Louie, and M. L. Cohen, Eu. Phys. Lett. **28** 335 (1994); Phys. Rev. B **51** 6868 (1995); A. Loiseau, F. Willaime, N. Demoncy, G. Hug, and H. Pascard Phys. Rev. Lett. **76** 4737 (1996).

[20] Y. Miyamoto, A. Rubio, S. G. Louie, and M. L. Cohen, Phys. Rev. B **50** 18360 (1994).

[21] Y. Miyamoto, A. Rubio, M. L. Cohen, and S. G. Louie, Phys. Rev. B **50** 4976 (1994).

[22] M. Damnjanović and M. Vujičić, Phys. Rev. B **25**, 6987 (1982).

[23] T. Vuković, I. Milošević, and M. Damnjanović, Phys. Lett. A **216** (1996) 307-12.

[24] J. Patera, R. T. Sharp, and P. Winternitz, J. Math. Phys. **19**, 2362 (1978); A. G. McLellan, J. Phys. C: Solid State Phys. **7**, 3326 (1974); J. Killinback, J. Phys. C: Solid State Phys. **5**, 2497 (1972).

[25] S. L. Altmann, *Band Theory of Solids. An introduction from the Point of View of Symmetry* (Clarendon Press, Oxford, 1991).

[26] I. Božović, M. Vujičić, and F. Herbut, J. Phys. A **11**, 2133 (1978); I. Božović, M. Vujičić, J. Phys. A **14**, 777 (1981).

[27] I. Milošević and M. Damnjanović, Phys. Rev., B **47** 7805 (1993).

[28] I. Božović, N. Božović, and M. Damnjanović, J. Phys. A **18** (1985) 923.

[29] M. Damnjanović, I. Milošević, and M. Vujičić, Phys. Rev. B **39** (1989) 4610; M. Damnjanović and I. Milošević, Phys. Rev. B **43** (1991) 13482.

SIMETRIJA NANOTUBA

M. Damnjanović, T. Vuković, I. Milošević

Zahvaljujući potencijalnim primenama u nanotehnologiji, nanotube su postale vrlo atraktivni predmet istraživanja u fizici čvrstog stanja. Zbog njihove naglašene simetrije, teorija grupe je važno sredstvo u teorijskom ispitivanju nanotuba. U ovom radu predstavljen je kratak pregled simetrijske analize fizike nanotuba.